doi:10.1093/brain/awq300 Brain 2010: 133; 3661–3675 | 3661

BRAIN
A JOURNAL OF NEUROLOGY

Multispectral brain morphometry in Tourette syndrome persisting into adulthood

Bogdan Draganski,[1,2,3,4] Davide Martino,[5] Andrea E. Cavanna,[6,7] Chloe Hutton,[2] Michael Orth,[8] Mary M. Robertson,[7] Hugo D. Critchley[9,10] and Richard S. Frackowiak[1,2,11]

1 Département des neurosciences cliniques, CHUV, University of Lausanne, CH-1011 Lausanne, Switzerland
2 Wellcome Trust Centre for Neuroimaging, University College London, Institute of Neurology, WC1N 3BG London, UK
3 Max Planck Institute for Human Cognitive and Brain Sciences, D-04103 Leipzig, Germany
4 Mind Brain Institute, Charité and Humboldt University, D-10099 Berlin, Germany
5 Department of Neurological and Psychiatric Sciences, University of Bari, I-70124 Bari, Italy
6 Department of Neuropsychiatry, University of Birmingham and BSMHFT, B15 2TT Birmingham, UK
7 Department of Mental Health Sciences, University College London, W1W 7EY London, UK
8 Department of Neurology, University Ulm, D-89081 Ulm, Germany
9 Psychiatry and Clinical Imaging Sciences Centre, Brighton & Sussex Medical School, University of Sussex Campus, BN1 9PX Brighton, UK
10 Neurobehavioural Clinic, Sussex Partnership NHS Foundation Trust, BN13 3EP Brighton, UK
11 Neuroimaging Laboratory, IRCCS Fondazione Santa Lucia, I-00179 Rome, Italy

Correspondence to: Bogdan Draganski,
Département des Neurosciences Cliniques,
CHUV, University of Lausanne,
Switzerland
E-mail: bogdan.draganski@gmail.com

Tourette syndrome is a childhood-onset neuropsychiatric disorder with a high prevalence of attention deficit hyperactivity and obsessive-compulsive disorder co-morbidities. Structural changes have been found in frontal cortex and striatum in children and adolescents. A limited number of morphometric studies in Tourette syndrome persisting into adulthood suggest ongoing structural alterations affecting frontostriatal circuits. Using cortical thickness estimation and voxel-based analysis of T1- and diffusion-weighted structural magnetic resonance images, we examined 40 adults with Tourette syndrome in comparison with 40 age- and gender-matched healthy controls. Patients with Tourette syndrome showed relative grey matter volume reduction in orbitofrontal, anterior cingulate and ventrolateral prefrontal cortices bilaterally. Cortical thinning extended into the limbic mesial temporal lobe. The grey matter changes were modulated additionally by the presence of co-morbidities and symptom severity. Prefrontal cortical thickness reduction correlated negatively with tic severity, while volume increase in primary somatosensory cortex depended on the intensity of premonitory sensations. Orbitofrontal cortex volume changes were further associated with abnormal water diffusivity within grey matter. White matter analysis revealed changes in fibre coherence in patients with Tourette syndrome within anterior parts of the corpus callosum. The severity of motor tics and premonitory urges had an impact on the integrity of tracts corresponding to cortico-cortical and cortico-subcortical connections. Our results provide empirical support for a patho-aetiological model of Tourette syndrome based on developmental abnormalities, with perturbation of compensatory systems marking persistence of symptoms into adulthood. We interpret the symptom severity related grey matter volume increase in distinct functional brain areas as evidence of ongoing structural plasticity. The convergence of evidence from volume and water diffusivity imaging strengthens the validity of our findings and attests to the value of a novel multimodal combination of volume and cortical thickness estimations that provides unique and complementary information by exploiting their differential sensitivity to structural change.

Received May 4, 2010. Revised August 27, 2010. Accepted September 6, 2010

Keywords: Tourette syndrome; voxel-based cortical thickness; voxel-based morphometry; mean diffusivity; fractional anisotropy

Abbreviations: ADHD = attention deficit hyperactivity disorder; OCD = obsessive-compulsive disorder; PUTS = premonitory urge for tics; VBM = voxel-based morphometry; YGTSS = Yale Global Tic Severity Scale

Introduction

Gilles de la Tourette's syndrome is a childhood-onset neuropsychiatric disorder with high heritability, characterized by tics i.e. rapid, non-rhythmic, stereotyped involuntary movements and vocalizations, involving virtually all body segments (Robertson, 2000). Although the majority of studies suggest an improvement of tic severity with adulthood in one-third of children with Tourette syndrome (Bloch and Leckman, 2009), a substantial proportion of patients remain symptomatic after the second decade of life (for review see Singer, 2005; Albin and Mink, 2006). Co-morbidities include obsessive-compulsive disorder (OCD), attention deficit hyperactivity disorder (ADHD) and antisocial behaviour (Cavanna *et al.,* 2009).

Our understanding of the predisposing factors for symptom persistence in adulthood, and their neuroanatomical correlates, remains limited. Basal ganglia dysfunction, encompassing altered dopaminergic regulation and abnormal motor and limbic fronto-striatal circuitry has been proposed as a pathophysiological basis for Tourette syndrome (Mink, 2003). Functional neuroimaging studies using either cognitive control or tic suppression paradigms support this hypothesis demonstrating increased compensatory neural activity in prefrontal cortex and striatum in both children and adults with Tourette syndrome compared with healthy volunteers (Peterson *et al.,* 1998; Serrien *et al.,* 2005; Baym *et al.,* 2008; Raz *et al.,* 2009; Mazzone *et al.,* 2010). The notion of dopaminergic hyperactivity in Tourette syndrome is illustrated, independently of motor behaviour, in cognitive paradigms including subliminal learning with and without dopamine blockade (Palminteri *et al.,* 2009). Nonetheless, precise knowledge about the neural circuitry involved in tic generation is limited by difficulties de-correlating functional (neuroimaging) activity prior to and during tics (Bohlhalter *et al.,* 2006).

To date, the majority of structural MRI studies in Tourette syndrome focus on children and adolescents, reflecting childhood onset and the peak of tic expression (for review on this topic see Plessen *et al.,* 2009). Manual and semi-automated region of interest volumetry analysis confirms predictions from clinical and theoretical disease models, by demonstrating structural changes in the basal ganglia, limbic structures and prefrontal cortex (Peterson *et al.,* 2001, 2003; Gerard and Peterson, 2003). Most studies employing a region of interest approach targeting the basal ganglia report volume decreases, notably with caudate hypoplasia in childhood correlating negatively with tic/OCD severity in adolescence (Peterson *et al.,* 1993, 2003; Bloch *et al.,* 2005). However, a recent study using a high-precision, surface-based diffeomorphic technique in neuroleptic-naïve adults with Tourette syndrome failed to show any significant volume or shape differences in the basal ganglia or thalamus (Wang *et al.,* 2007). Mesial temporal 'limbic' structures reportedly show a strong age-dependency, with larger hippocampus and amygdala volumes in children with Tourette syndrome and smaller ones in adults with Tourette syndrome (Peterson *et al.,* 2007). Prefrontal cortex and parietal region of interest analyses reveal similar age-dependent changes and negative correlations with tic severity, which suggests ongoing anatomical alterations in Tourette syndrome brains (Peterson *et al.,* 2001). According to a recent region of interest study in children and adults with Tourette syndrome, there is a disease-related volume reduction of the cerebellum that correlates with tic severity and motor disinhibition. Interestingly, the correlation with OCD severity showed reversed directionality of changes with cerebellar volume increases in patients with Tourette syndrome with OCD co-morbidity (Tobe *et al.,* 2010).

Computational neuroanatomy on magnetic resonance images is a validated approach for unbiased investigation of brain structural correlates of neurological and psychiatric disorders (Ashburner *et al.,* 2003). The few published studies on Tourette syndrome using a voxel-based morphometry (VBM) whole-brain approach report differences from normal subjects within the basal ganglia, limbic system and prefrontal cortex, corroborating region of interest volumetry results (Ludolph *et al.,* 2006; Muller-Vahl *et al.,* 2009). Mesencephalic grey matter expansion in Tourette syndrome is a novel finding identified by VBM, lending support for Devinsky's hypothesis of abnormal function in mesencephalic structures (Garraux *et al.*, 2006). VBM analysis of diffusion-weighted images in Tourette syndrome has demonstrated cerebral white matter fibre coherence changes underneath the left sensorimotor cortex that correlated with tic severity (Thomalla *et al.,* 2009). Moreover, findings from a diffusion-weighted imaging-based probabilistic tractography study of children with Tourette syndrome seem to have captured fine-grained anatomical connectivity differences within frontostriatal circuits (Makki *et al.,* 2009).

Assessment of cortical thickness calculated either from surface- (Fischl *et al.,* 1999) or voxel-based (Hutton *et al.,* 2008, 2009) identification of grey/white matter boundaries offers a complementary perspective for morphological exploration of brain structure changes between healthy and diseased brains (Winkler *et al.,* 2009). Recent cortical thickness studies in children and adolescents with Tourette syndrome show a loss of cortical grey matter in ventral frontal and sensorimotor cortices (Sowell *et al.,* 2008; Fahim *et al.,* 2009). The reported cortical thinning depends on patient age and is correlated negatively with worst-ever tic severity.

In this study, we focused on structural brain changes in a specific well-defined disease population i.e. adult patients with Tourette syndrome. We hypothesized persisting morphological abnormalities in cortical and subcortical regions representing nodes in dysfunctional limbic and sensorimotor frontostriatal circuits (Plessen *et al.,* 2009). We adopted a multimodal strategy acquiring T1-weighted and diffusion-weighted imaging data in order to characterize both grey matter volume and white matter integrity. Besides the established VBM technique we used the newly developed voxel-based approach for cortical thickness assessment (Hutton *et al.,* 2009).

The voxel-based cortical thickness method captures only changes in cortical thickness, whereas VBM infers both cortical folding abnormalities and cortical/subcortical grey matter volume differences. We anticipated that the complementary character of both voxel-based techniques would allow more straightforward interpretation between cortical folding abnormalities and grey matter tissue loss.

Materials and methods

Participants

Forty adult patients with Tourette syndrome (mean age 32.4 ± 11 years, range 18–56 years, 10 female) were consecutively recruited from the specialist Tourette syndrome outpatient clinic at the National Hospital for Neurology and Neurosurgery, London. Patients were included in the study if they met full DSM-IV-TR (Diagnostic and Statistical Manual of Mental Disorders, Fourth Edition) criteria for Gilles de la Tourette's syndrome, and required periodic follow-up at the outpatient clinic at the time of the study. Forty healthy adult volunteers (mean age 34.4 ± 9 years, range 19–58 years, 15 female) were recruited as a control group (Table 1); inclusion in the control group required the absence of a tic disorder, ADHD or OCD in accordance with DSM-IV-TR criteria. All relevant demographic and clinical details of the study participants are summarized in Table 1. We excluded six patients and eleven controls from the diffusion-weighted imaging analysis due to movement artefacts. Exclusion criteria for both groups included epilepsy, lifetime substance abuse, developmental delay, psychosis and head trauma with loss of consciousness, prior brain, spinal or peripheral nerve surgery and structural abnormalities on visual inspection of conventional T1-weighted magnetic resonance images. After a complete description

Table 1 Demographic and clinical details of the study participants

Patient	Sex	Age	Age at tic onset	Motor tics	Vocal tics	YGTSS	OCD	ADHD	Medication
1	F	20	8	11	5	19	No	No	Nil
2	F	44	5	6	2	26	No	No	Nil
3	M	16	4	25	5	26	No	Yes	Nil
4	F	29	5	7	4	24	No	No	Nil
5	M	21	10	30	7	37	Yes	Yes	Nil
6	M	24	5	26	10	25	No	No	Nil
7	M	20	7	17	5	27	No	No	Nil
8	F	36	3	18	12	31	No	No	Nil
9	F	24	7	15	1	30	No	No	Nil
10	M	38	10	23	3	25	Yes	No	Nil
11	M	47	6	43	3	24	No	Yes	Nil
12	M	17	6	66	13	21	Yes	No	Nil
13	M	33	7	21	5	22	No	No	Nil
14	M	33	7	11	2	21	No	No	Nil
15	F	35	9	10	10	35	No	No	Nil
16	M	55	15	20	2	31	Yes	Yes	Paroxetine
17	F	37	5	35	5	14	Yes	No	Paroxetine
18	F	66	3	7	3	17	No	Yes	Paroxetine
19	M	31	13	9	2	28	Yes	Yes	Citalopram, Zopiclone
20	M	19	7	16	5	28	No	No	Clonidine
21	M	32	9	26	9	36	Yes	No	Fluoxetine
22	M	18	6	19	3	20	Yes	Yes	Clonidine
23	M	31	7	18	6	33	No	Yes	Risperidone
24	F	23	2	26	14	40	No	No	Haloperidol, Fluoxetine
25	M	39	5	21	15	33	No	No	Sulpiride
26	F	29	9	36	15	35	Yes	No	Haloperidol, Cipramil, Procyclidine
27	M	26	11	36	9	37	No	Yes	Risperidone
28	M	22	6	30	12	43	No	No	Pimozide, Fluoxetine
29	M	33	5	4	3	23	No	Yes	Sulpiride, Clomipramine
30	M	51	6	26	11	42	No	Yes	Sulpiride
31	M	21	7	14	3	14	No	Yes	Sulpiride, Risperidone, Amitriptyline
32	M	19	6	19	5	24	Yes	Yes	Sulpiride, Clonidine, Risperidone
33	M	50	7	32	8	29	Yes	No	Risperidone, Fluoxetine
34	M	18	4	42	22	39	No	Yes	Risperidone
35	M	24	8	5	3	35	Yes	Yes	Depixol
36	M	41	8	45	21	32	No	Yes	Haloperidol
37	M	21	3	39	9	22	No	Yes	Risperidone
38	M	38	7	14	3	30	No	No	Venlafaxine, Quetiapine
39	M	33	8	28	10	34	Yes	Yes	Sulpiride, Diazepam, Fluoxetine
40	M	33	6	13	12	35	Yes	Yes	Risperidone

F = female; M = male.

of the study, informed consent was obtained from all participants according to the Declaration of Helsinki, the Joint Medical Ethics Committee of the National Hospital for Neurology and Neurosurgery and the Institute of Neurology approved the study.

Lifetime and current clinical information was systematically collected using clinical assessment and structured instruments within a time interval of 3 months from MRI. All clinical evaluations were performed by a board-certified consultant psychiatrist (H.D.C.) and a board-certified neurologist (A.E.C.), both with extensive experience in the diagnosis of Tourette syndrome. Diagnoses were further verified by a senior neuropsychiatrist (M.M.R.) and neurologist (M.O.). Clinical diagnoses were assigned only when there was full consensus between the examining physician and the two senior clinicians.

The National Hospital Interview Schedule for Gilles de la Tourette's syndrome was used to summarize specific and detailed information about motor and phonic tics and the Yale Global Tic Severity Scale (YGTSS; Leckman *et al.,* 1989) was used to assess current tic severity. Mean disease duration was 24 ± 11.6 years; mean age at onset was 6.8 ± 2.6 years. Nineteen patients (47.5%) were diagnosed with ADHD and 14 (35%) with OCD. Eight patients (20%) had both ADHD and OCD co-morbidities. Twenty-five patients (62.5%) reported the occurrence of premonitory sensations prior to motor/vocal tics; the mean YGTSS was 28.7 ± 7.4 (mean ± standard deviation), the mean motor tic subscore: 22.7 ± 13, the mean Premonitory Urge for Tics (PUTS; Woods *et al.,* 2005) score: 21.5 ± 7.4 and the mean Leyton Obsessional Inventory (Cooper, 1970) score: 25.6 ± 13.6. Fifteen patients (37.5%) were medication naïve, 7 (17.5%) took antidepressants (mainly selective serotonin reuptake inhibitors) and 18 (45%) were prescribed atypical neuroleptics (Table 1).

Data acquisition

MRI was performed on a Siemens Sonata scanner (Erlangen, Germany) operating at 1.5 T using a phased-array coil and two imaging protocols: (i) T1-weighted 3D Modified Driven Equilibrium Fourier Transform (MDEFT) protocol (176 slices, 1 mm thickness, in-plane resolution 1 mm, no interslice gap, sagittal acquisition, phase encoding in anterior/posterior direction, field of view 224 × 256 mm, matrix 224 × 256, repetition time = 20.66 ms, echo time = 8.42 ms, inversion time = 640 ms, flip angle 25°, fat saturation, bandwidth 178 Hz/pixel); and (ii) diffusion-weighted imaging protocol (echo-planar sequence with a double spin-echo module to reduce the effect of eddy currents (Reese *et al.,* 2003), 40 axial slices of 2.3 mm thickness, with no inter-slice gaps and an acquisition matrix of 96 × 96 in a field of view of 220 × 220 mm^2, resulting in 2.3 mm^3 isotropic voxels, inter-slice temporal separation = 155 ms, echo time = 90 ms, flip angle 90°, fat saturation, bandwidth 2003 Hz/pixel, 61 high diffusion-weighted images (b = 1000 s/mm^2), seven low-diffusion-weighted images (b = 100 s/mm^2). Data acquisition was cardiac gated to reduce motion artefacts due to pulsation of the cerebrospinal fluid (Wheeler-Kingshott *et al.,* 2002).

Processing of structural data

Data pre-processing and analysis were performed with SPM8 software (Wellcome Trust Centre for Neuroimaging, London, UK, http://www.fil.ion.ucl.ac.uk/spm) running under MATLAB 7 (Mathworks, Sherborn, MA, USA). T1-weighted scans were partitioned automatically into different tissue classes—grey matter, white matter and non-brain (CSF, skull), using the 'unified segmentation' approach (Ashburner and Friston, 2005). For optimal registration of the brains of different subjects, scans were normalized to a population template generated from the complete data set using a diffeomorphic registration algorithm (Ashburner, 2007). This high-dimensional, non-linear warping algorithm selects conserved features, which are informative for registration, thus minimizing structural variation among subjects and providing optimal inter-subject registration. Subsequently, all images were scaled by the Jacobian determinants from the normalization step to preserve initial volumes (Good *et al.,* 2001) and smoothed by convolution with an isotropic Gaussian kernel of 6 mm full-width at half maximum.

We created a voxel-based cortical thickness map for each individual using the grey matter, white matter and CSF tissue partitions created in the previous step. For this, we used the recently optimized voxel-based cortical thickness method that allows automated extraction of cortical grey matter boundaries from T1-weighted images and measurement of cortical thickness at each voxel (Hutton *et al.,* 2009). Subsequently, the voxel-based cortical thickness maps were registered to the common standardized space using the deformation fields applied for grey matter warping. The warped voxel-based cortical thickness maps were then smoothed by convolution with an isotropic Gaussian kernel of 6 mm full-width at half maximum using a modified weighted smoothing procedure described below.

Diffusion tensor imaging scalar parameters (fractional anisotropy and mean diffusivity) were computed with Camino software (www.cs.ucl.ac.uk/research/medic/camino) (Cook *et al.,* 2005). For automated motion correction in statistical parametric maps, we used images without diffusion weighting and rigid-body transformations. We fitted the diffusion tensor using the standard linear least squares fit to the log measurements (Basser *et al.,* 1994). After affine registration of diffusion tensor imaging data to the white matter tissue class based on T1-weighted images we performed non-linear registration using parameter estimates from the grey matter registration step similar to the warping procedure for cortical thickness.

We implemented a modified weighted smoothing procedure to compensate for the effect of Gaussian smoothing on the original cortical thickness/diffusion tensor imaging parameter values. The Gaussian smoothing kernel, which is applied in standardized space, was transformed back into subject native space while preserving the averaged cortical thickness/diffusion tensor imaging parameter value over a region the size of the smoothing kernel. A similar approach has been previously applied to voxel-based analysis of cortical thickness and diffusion tensor imaging (Hutton *et al.,* 2009; Lee *et al.,* 2009):

$$signal = \frac{g * (ws(\phi))}{g * w}$$

where $s(\phi)$ is the warped by ϕ parameter map (cortical thickness map, fractional anisotropy or mean diffusivity); $g*$ indicates convolution with the Gaussian smoothing kernel; w represents the weights, constructed from $w = |D\phi|t(\phi)$ with $|D\phi|$, the Jacobian determinants of deformation ϕ and $t(\phi)$, the tissue class image warped by ϕ.

Data analysis

Regional differences between patients with Tourette syndrome and controls were examined by creating separate voxel-by-voxel whole-brain statistical parametric maps based on the smoothed warped grey matter segments, voxel-based cortical thickness maps, fractional anisotropy/mean diffusivity grey and white matter images using the General Linear Model and Random Field Theory. Total intracranial volume was calculated for each individual by summing together voxel values of the grey matter, white matter and CSF segmented images in native space.

Group analysis

For group analysis, we used an ANOVA design with factors co-morbidity (OCD: presence or absence; ADHD: presence or absence) and diagnosis (Tourette syndrome and controls). We tested for main effects of diagnosis (Tourette syndrome versus controls) and interactions with co-morbidity (OCD, ADHD). Age, gender and total intracranial volume were included in the design matrix to control for any independent effects of these covariates on our findings. Gender effects and the impact of medication status (three levels—no medication, antidepressants, neuroleptics) were tested in the same model.

Correlation analysis with symptom severity

We tested for main effects/interactions between symptom severity (YGTSS, motor tic sub-score, PUTS, Leyton Obsessional Inventory score) and co-morbidities (OCD, ADHD) using a similar model but without the control group. Age, gender and total intracranial volume were also included as regressors in the design matrix.

Correlation analysis between volume and thickness

To determine the relationship between grey matter volume and cortical thickness at the voxel level, we adopted the approach used by Josse *et al.* (2008). Individual grey matter volumes entered the design matrix as dependent variables, voxel-based cortical thickness data were used as regressors in addition to age, gender and total intracranial volume. We fitted the regression model to the grey matter volume images using the classical General Linear Model implemented in statistical parametric maps. The smoothness of the images was derived from the residuals and random field theory was applied to compute *P*-values corrected for search volumes.

Statistical inference and thresholds

First, we computed summary statistics (e.g. contrasts) and *t*/*F* values at the voxel level throughout the brain without restriction of the search volume. In order to increase analytical sensitivity with respect to frontal/parietal cortex, limbic regions and basal ganglia as candidate regions for brain structural abnormalities in Tourette syndrome that persists into adulthood (Plessen *et al.*, 2009), we restricted our search volume for grey matter analysis to the subset of *a priori* postulated anatomical areas as defined by an automated anatomical labelling atlas (Tzourio-Mazoyer *et al.*, 2002) after using an auxiliary uncorrected voxel threshold of $P < 0.001$ (Friston *et al.*, 1994). For white matter analysis, we adopted the same strategy, using an anatomical mask restricted to the corpus callosum and corticostriatal subcortical areas (Plessen *et al.*, 2009). For *a priori* hypotheses in pre-specified regions the threshold was set at $P < 0.05$ after Family Wise Error correction for multiple comparisons in small volumes (small volume correction) (Worsley *et al.*, 1996; Friston, 1997). To further characterize interactions with co-morbidity and the direction of these effects, we extracted regression coefficients (betas) centred on the local voxel maxima and present them graphically next to the corresponding contrasts (Figs 1–4).

Results

Clinical assessment

Testing for interactions between co-morbidity (OCD or ADHD) and symptom severity failed to reveal significant results [overall tic severity (YGTSS), $P = 0.45$; motor tic sub-score, $P = 0.1$; or premonitory sensation intensity (PUTS), $P = 0.47$]. Also there was no significant interaction between gender and symptom severity [overall tic severity (YGTSS), $P = 0.97$; motor tic sub-score, $P = 0.09$; premonitory sensation intensity (PUTS), $P = 0.46$]. For obsessive-compulsive symptom severity (Leyton Obsessional Inventory score) we show a significant effect of co-morbidity (OCD: $P < 0.0001$) without significant effect of gender ($P = 0.3$).

Grey matter analysis

Group analysis

There was no significant difference between total intracranial volumes comparing patients with Tourette syndrome and healthy controls ($P = 0.25$).

Adults with Tourette syndrome compared with controls showed significant grey matter volume decreases in the medial orbitofrontal, rostral cingulate, ventrolateral prefrontal cortex and operculum paralleled by volume increase in the putamen bilaterally (Fig. 1, Table 2). We demonstrate a concomitant mean diffusivity increase in orbitofrontal cortex for the Tourette syndrome cohort (Table 2). Additionally, there was a significant Group × Age interaction in rostral anterior cingulate cortex such that patients with Tourette syndrome showed a greater negative correlation with age than controls (Table 2).

In the Tourette syndrome cohort, the cortical thickness analysis revealed significant thinning in mesial temporal 'limbic' areas—amygdala and hippocampus; additionally there was thinning in orbitofrontal cortex, ventrolateral prefrontal cortex and bilateral operculum (Fig. 2A, Table 4). Further, we observed increased cortical thickness in primary somatosensory cortex and right dorsal premotor cortex (Fig. 2B and Table 4).

Effect of co-morbidity

An analysis of grey matter volume and cortical thickness identified significant grey matter decreases in the left inferior parietal cortex and posterior hippocampus bilaterally as the main effect of ADHD co-morbidity (Fig. 3A, Tables 2 and 4). There were no grey matter changes associated with the presence or absence of OCD.

Symptom severity correlation analysis

The VBM analysis failed to demonstrate any significant correlation between grey matter volume and overall tic severity (YGTSS). However, YGTSS was negatively correlated with cortical thickness in orbitofrontal cortex and bilateral ventrolateral prefrontal cortex (Table 4). We detected significant positive correlation between fractional anisotropy values in the caudate body bilaterally and tic severity (Table 3).

There were no significant correlations between grey matter parameters and the motor tic sub-score. The intensity of premonitory

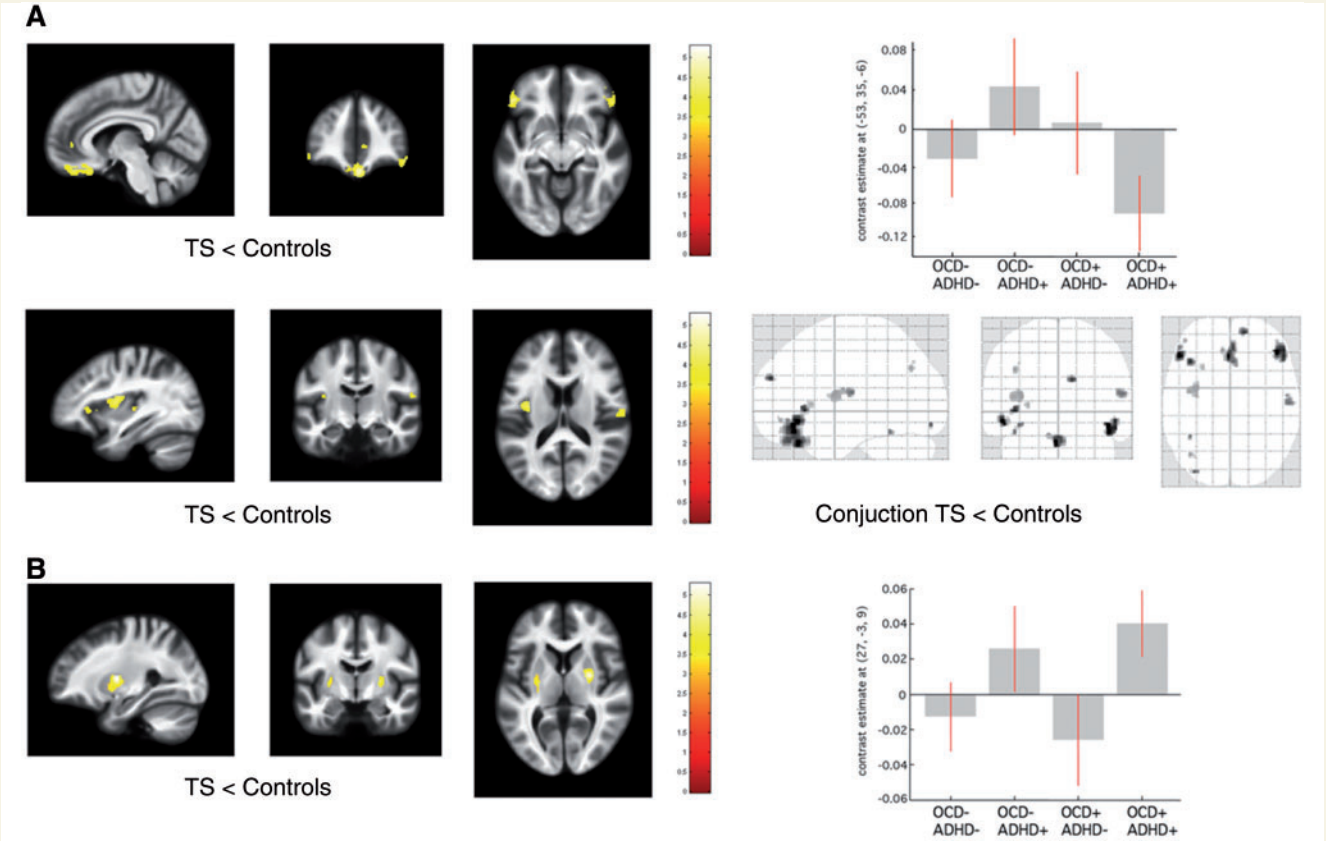

Figure 1 Statistical parametric maps of significant grey matter volume change in the Tourette syndrome cohort superimposed for presentation purposes at $P < 0.001$, uncorrected, on T1-weighted image. *Right panel*: box-plots of regression coefficients (betas) extracted from the voxel of maximum intensity over Tourette syndrome sub-groups depending on the presence (+) or absence (−) of co-morbidity OCD/ADHD (red bars indicating 90% confidence interval); 'glass brain' with the result of the conjunction analysis. (**A**) Grey matter volume decrease in patients with Tourette syndrome (TS) compared with controls. (**B**) Grey matter volume increase in patients with Tourette syndrome compared with controls. [*x*, *y*, *z*] coordinates refer to the Montreal Neurological Institute space. Colour scales on the right indicate *t*-values.

urges for tics (PUTS) showed significant positive correlation with grey matter volume and cortical thickness in the left somatosensory cortex and the prefrontal cortex (Fig. 3B, Tables 3 and 4).

Symptom severity: interaction with gender, co-morbidities and medication

Further exploration of the correlation between grey matter volume/cortical thickness and YGTSS tested for interaction with the factor co-morbidity. The voxel-based cortical thickness analysis showed a negative correlation between orbitofrontal cortex/ventrolateral prefrontal cortex thickness and YGTSS only for ADHD positive patients with Tourette syndrome (Table 4). The polarity of correlation between orbitofrontal cortex thickness and YGTSS in patients with Tourette syndrome with OCD depended on the presence of ADHD as a second co-morbidity factor such that patients with Tourette syndrome with 'OCD only' showed a positive correlation. Additionally, we detected a negative correlation between ventral striatal volume (nucleus accumbens) and obsessive-compulsive symptom severity assessed with the Leyton Obsessional Inventory score (Fig. 3A and Table 3).

There were no further significant interactions between cortical thickness/grey matter volume and gender or medication status. We report descriptively a trend towards ventral striatal volume increases in adults with Tourette syndrome on neuroleptic medication.

White matter analysis

Group analysis

Group comparisons revealed a significant fractional anisotropy decrease in the genu of the corpus callosum in the Tourette syndrome cohort compared with controls (Fig. 4A and Table 2). We observed a fractional anisotropy increase with a mean diffusivity decrease in the somatosensory cortex region bilaterally in patients with Tourette syndrome (Table 2).

Effect of co-morbidity

There was a negative correlation between the motor tic sub-score and fractional anisotropy values in the frontal portion of the superior longitudinal fascicle bilaterally (Fig. 4B and Table 3).

Table 2 Summary of VBM results over cohorts ($P_{Family\text{-}wise\ error} < 0.05$ after small volume correction)

VBM analysis	Region	Left hemisphere coordinates (mm)			t-score	z-score	Right hemisphere coordinates (mm)			t-score	z-score
		x	y	z			x	y	z		
T1-weighted grey matter											
Tourette syndrome < controls	VLPFC	−53	35	−6	4.8	4.5	45	38	−12	4.9	4.5
	OFC						0	33	−26	5.3	4.8
	Operculum	−39	−3	7	4.4	4.1	58	−13	16	3.9	3.7
	rACC						7	44	1	3.7	3.6
Tourette syndrome > controls	Putamen	−27	−10	3	3.3	3.2	27	−3	9	4.5	4.2
Interaction Group × Age tourette syndrome < controls	rACC						5	45	0	4.8	4.4
ADHD+<ADHD−	Hippocampus	−23	−33	0	4.6	4.3	24	−36	0	3.6	3.5
	IPC	−60	−46	25	4.4	4.11					
Mean diffusivity grey matter											
Tourette syndrome > controls	OFC						9	29	−24	3.9	3.7
Fractional anisotropy grey matter											
Tourette syndrome > controls	SI	−17	−37	64	3.1	2.9	27	−45	54	5	4.5
Fractional anisotropy white matter											
Tourette syndrome < controls	CC						3	21	−3	4.5	4.1
Mean diffusivity white matter											
Tourette syndrome < controls	SI	−21	−30	70	3.4	3.2	10	−37	70	3.3	3.1

Coordinates [*x*, *y*, *z*] refer to the Montreal Neurological Institute (MNI) standard stereotactic space.
rACC = rostral anterior cingulate cortex; CC = corpus callosum; IPC = inferior parietal cortex; OFC = orbitofrontal cortex; SI = primary somatosensory cortex; VLPFC = ventrolateral prefrontal cortex.

Fractional anisotropy values in the parietal portion of superior longitudinal fascicle were negatively correlated with the intensity of premonitory urges (Fig. 4B and Table 3).

Tic severity: interaction with gender, co-morbidity and medication

Medication use and co-morbidities had no further modulatory effect on the correlation between white matter micro-structural integrity and symptom severity.

Voxel-based morphometry versus voxel-based cortical thickness: voxel-by-voxel correlation analysis

The regression between voxel-based cortical thickness and VBM demonstrated that grey matter volume was positively predicted by cortical thickness. The positive relationship was observed in the majority of cortical regions showing Tourette syndrome-related changes *per se* (Supplementary Fig. 1). At a lower threshold ($P < 0.001$ uncorrected), we found negative correlations between voxel-based cortical thickness and VBM in the regions of the superior frontal gyri and around the ventricles.

Discussion

In our study of a relatively large cohort of patients with Tourette syndrome persisting into adulthood, we observed a characteristic pattern of brain structural changes across regions implicated in attentional, motivational, cognitive and somatosensory processing. Our findings with grey matter volume/cortical thickness decrease in prefrontal and limbic structures provide empirical validation for the hypothesis of dysfunctional frontostriatal circuits in Tourette syndrome. Somatosensory cortex expansion associated with higher premonitory sensation intensity, however, can be seen as evidence for ongoing neural plasticity. Additionally, we detected abnormalities in white matter fibre integrity within corpus callosum and in subcortical white matter tracts corresponding to frontal and parietal portions of superior longitudinal fascicle. The structural brain changes are further modulated by the symptom severity and the presence of co-morbidities (ADHD and OCD). Based on two complementary voxel-based analysis techniques for cortical thickness and grey matter volume additionally to fibre orientation/water diffusivity assessment, our results allow for a more confident and comprehensive interpretation of morphological changes suggesting anatomically evident pathology in frontostriatal circuits paralleled by plastic changes in primary somatosensory cortical areas.

Affected network nodes

Our findings show a distinct pattern of brain structure changes affecting mainly the limbic frontostriatal circuitry, extending further to networks related to sensorimotor function.

Prefrontal areas

Adults with Tourette syndrome demonstrate grey matter decrease in areas of the prefrontal cortex known to regulate together with the basal ganglia goal-directed behaviour (Haber and Knutson, 2010). Specifically, the orbitofrontal cortex is a structure involved in adaptive decision-making through its function in the

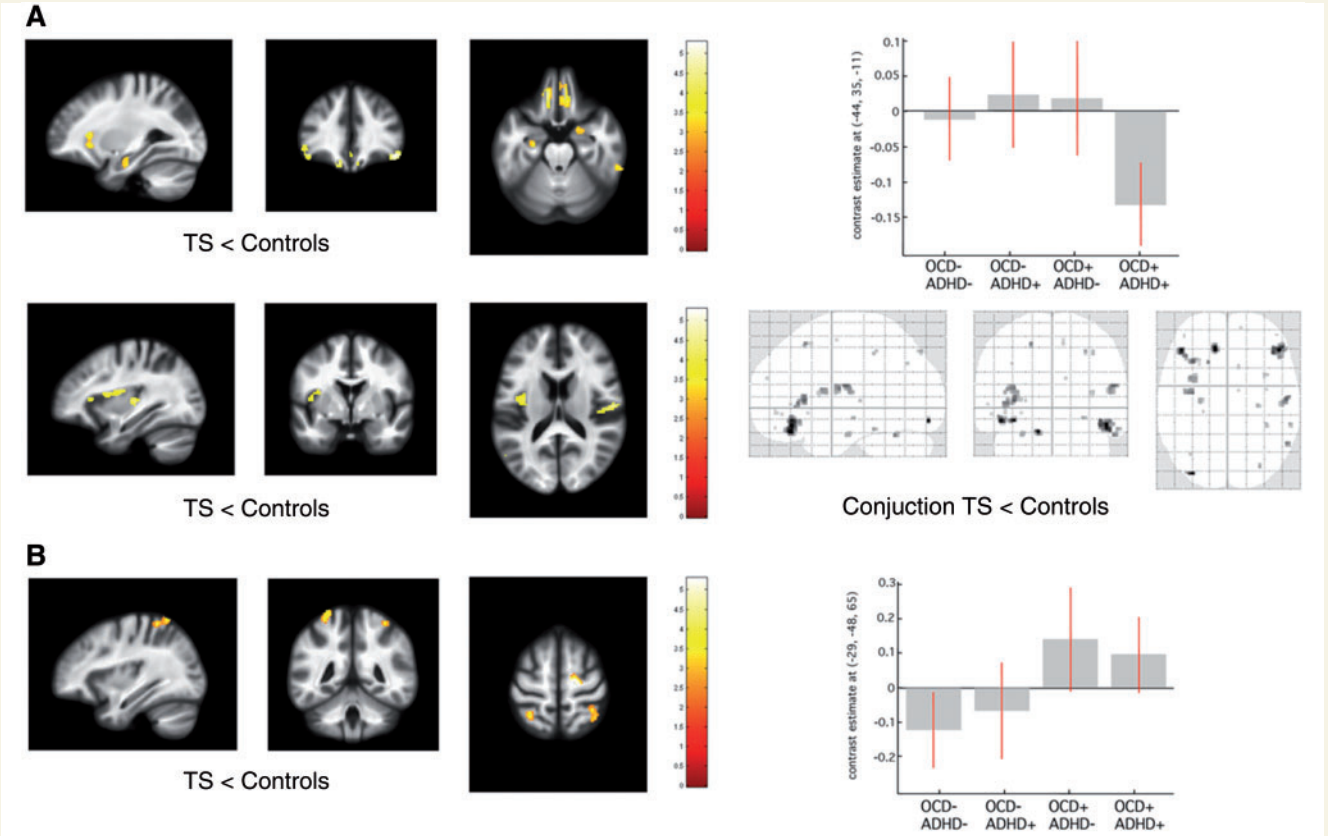

Figure 2 Statistical parametric maps of significant cortical thickness change in the Tourette syndrome cohort superimposed for presentation purposes at $P < 0.001$, uncorrected on T1-weighted image. *Right panel*: box-plots of regression coefficients (betas) extracted from the voxel of maximum intensity over Tourette syndrome (TS) sub-groups depending on the presence (+) or absence (−) of co-morbidity OCD/ADHD (red bars indicating 90% confidence interval); 'glass brain' with the result of the conjunction analysis. (**A**) Cortical thickness decrease in patients with Tourette syndrome compared with controls. (**B**) Cortical thickness increase in patients with Tourette syndrome compared with controls. [*x*, *y*, *z*] coordinates refer to the Montreal Neurological Institute standardized space. Colour scales on the right indicate *t*-values.

representation of value and reward (Schultz, 2004). Dysfunction of orbitofrontal cortex, as suggested by a persistent volume/thickness reduction in adults with Tourette syndrome, could explain deficits in the flexible control of behaviour (O'Doherty *et al.*, 2007). Together with orbitofrontal areas, related prefrontal structures like ventrolateral prefrontal cortex are believed to play a pivotal role in behavioural inhibition and impulse control (Hesslinger *et al.*, 2002; Aron *et al.*, 2003). Our findings corroborate a previous study associating tic severity in adults with Tourette syndrome with regional cortical thinning in orbitofrontal regions (Peterson *et al.*, 2001).

Limbic structures

The 'limbic' structures anterior cingulate cortex, hippocampus and amygdala represent that part of the frontostriatal Tourette syndrome matrix linked directly to the ventral striatum where motivational and incentive behaviours are regulated (Haber and Knutson, 2010). In-line with previous findings (Ludolph *et al.*, 2006; Peterson *et al.*, 2007) we observe cortical thinning in hippocampus and amygdala, highlighting the greater sensitivity of the voxel-based cortical thickness method for detecting structural abnormalities in these anatomical areas. Hippocampus and orbitofrontal cortex also show strong reciprocal connections (Ramus *et al.*, 2007) suggesting, through the observed parallel structural changes a disruption of specific network involved in anticipation, evaluation and learning. According to our hypothesis, VBM changes in the absence of cortical thickness correlates can be interpreted as a cortical folding abnormality, although the underlying pathophysiological process and its exact behavioural impact remain elusive.

Basal ganglia

Our results show a volume increase in the dorsolateral putamen in adults with Tourette syndrome compared with controls, mainly driven by the presence of ADHD co-morbidity (Fig. 1). Dorsolateral putamen has an important role in motor planning through predominant projections to sensorimotor areas (Alexander *et al.*, 1990; Draganski *et al.*, 2008). Further, we demonstrate ventral striatal atrophy in patients with Tourette syndrome with OCD and fractional anisotropy increases in the body of the caudate correlating with overall tic severity. Hypothetically, pathological increase in motor activity due to tics and increased sensory input caused by premonitory sensations could induce, via neural plasticity mechanisms, a volume expansion of the

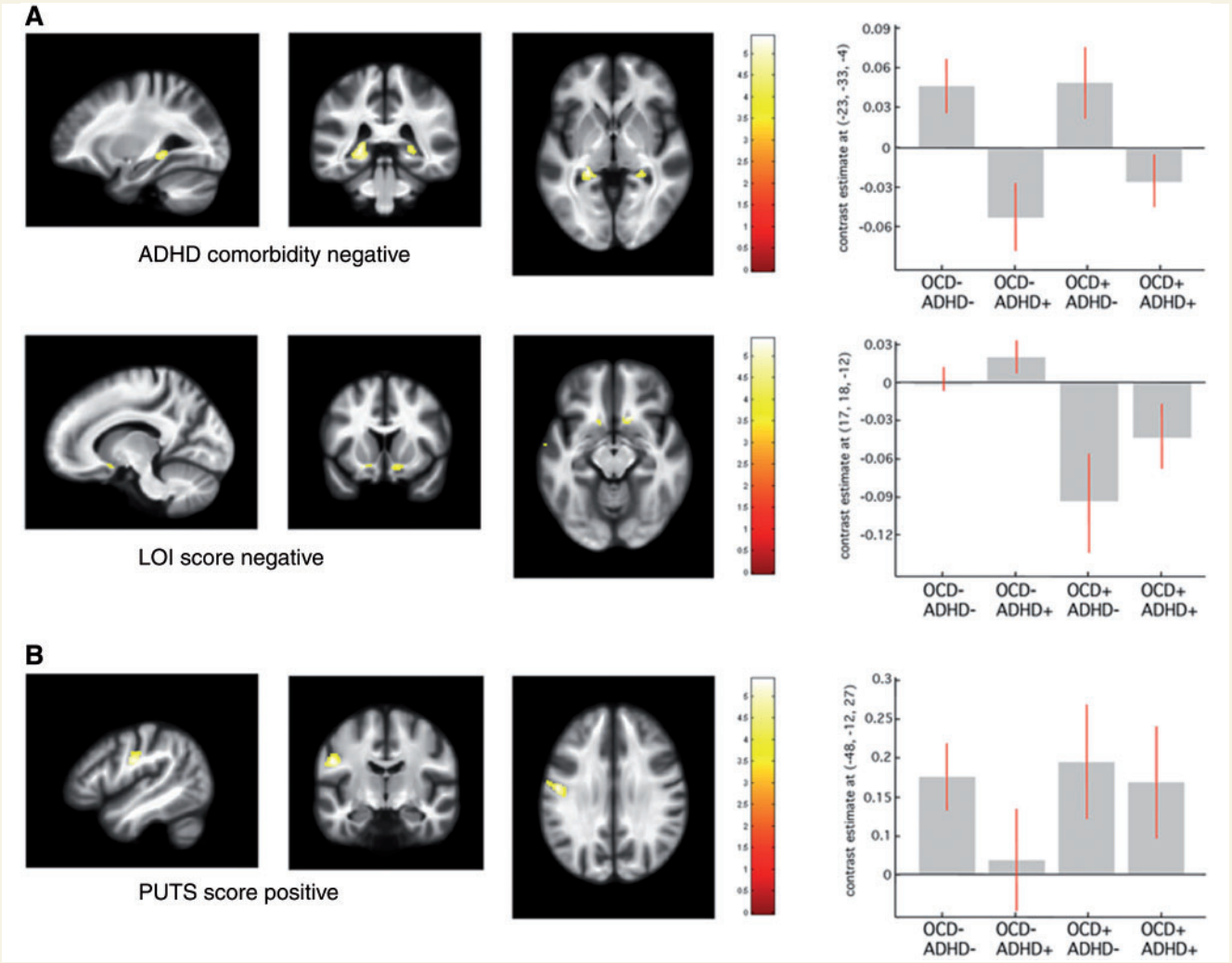

Figure 3 Statistical parametric maps of significant grey matter volume change in the Tourette syndrome cohort superimposed for presentation purposes at $P < 0.001$, uncorrected on T1-weighted image. *Right panel*: regression coefficients (betas) extracted from the voxel of maximum intensity over Tourette syndrome sub-groups depending on the presence (+) or absence (−) of co-morbidity OCD/ADHD. (**A**) Grey matter volume reductions in patients with Tourette syndrome with ADHD and with obsessive-compulsive symptom severity increase [Leyton Obsessional Inventory (LOI) score]. (**B**) Grey matter volume expansions in patients with Tourette syndrome with symptom severity increase [premonitory urge for tics score (PUTS)]. [*x*, *y*, *z*] coordinates refer to the Montreal Neurological Institute standardized space. Colour scales on the right indicate *t*-values.

dorsolateral putamen. The absence of correlation with tic severity and a weak trend for interaction with severity of premonitory urges do not lend strong support to this hypothesis. It is important to note that this result is discordant with a previous region of interest study showing striatal volume decreases in adults with Tourette syndrome (Peterson *et al.*, 1993, 2003). However, the main effect in striatum described by Peterson *et al*., was driven by a volume decrease in the caudate, a structure with marginal contribution to sensorimotor cortico-subcortical loops compared with putamen (Parent and Hazrati, 1995). Besides a difference in methodology and subject characteristics, we speculate that the presence of neuroleptic therapy could also be responsible for increased striatal volume, as suggested by previous studies (Peterson *et al.*, 2007) and in accord with our own findings that show a trend for striatal expansion in neuroleptics-treated patients with Tourette syndrome.

Somatosensory cortex

The observed grey matter increase in primary somatosensory cortex in adults with Tourette syndrome correlated positively with the intensity of premonitory sensations. The validity of our cortical thickness findings is further supported by fractional anisotropy changes in subcortical white matter corresponding to somatosensory cortex projections (Eickhoff *et al.*, 2005). Similar to a previous report on white matter structure change in somatosensory cortex published by Thomalla *et al*. (2009), we demonstrate mean diffusivity decrease in the same areas. According to combined diffusion tensor imaging/histology studies in animals

Table 3 Summary of VBM results—regression with clinical scores ($P_{Family\text{-}wise\ error} < 0.05$ after small volume correction)

VBM analysis	Region	Left hemisphere coordinates (mm)			*t*-score	*z*-score	Right hemisphere coordinates (mm)			*t*-score	*z*-score
		x	*y*	*z*			*x*	*y*	*z*		
T1-weighted grey matter—regression											
LOI score											
OCD—negative correlation	NAcc	−14	11	−14	4.1	3.6	16	18	−12	5.1	4.3
PUTS											
Tourette syndrome—positive correlation	SI	−48	−12	27	5.1	4.3					
	PFC						21	26	42	4.7	4
	PMd	−57	−4	37	5.2	4.3					
Fractional anisotropy grey matter—regression											
YGTSS											
Tourette syndrome—positive correlation	Caudate	−14	0	15	5	4.2	18	−4	15	5.1	4.3
Fractional anisotropy white matter—regression											
Motor tic sub-score											
Tourette syndrome—negative correlation	SLF II	−20	0	33	4.8	4	30	8	18	5.4	4.3
PUTS											
Tourette syndrome—negative correlation	SLF I	−27	−63	22	5.9	4.6	27	−55	22	5.7	4.5
	SLF II	−23	9	27			21	14	31	5	4

Coordinates [*x*, *y*, *z*] refer to the Montreal Neurological Institute (MNI) standard stereotactic space.
LOI = Leyton Obsessional Inventory; NAcc = nucleus accumbens; PMd = dorsal premotor cortex; PFC = prefrontal cortex; SLF = superior longitudinal fascicle I, II or III; SI = primary somatosensory cortex.

Table 4 Summary of voxel-based cortical thickness results ($P_{Family\text{-}wise\ error} < 0.05$ after small volume correction)

Voxel-based cortical thickness analysis	Region	Right hemisphere coordinates (mm)			*t*-score	*z*-score	Right hemisphere coordinates (mm)			*t*-score	*z*-score
		x	*y*	*z*			*x*	*y*	*z*		
T1-weighted grey matter											
Tourette syndrome > controls	SI	−29	−48	64	3.5	3.4	35	−45	61	3.6	3.5
	PMd						18	−15	62	4	3.7
Tourette syndrome < controls	OFC	−12	35	−21	4.1	4					
	VLPFC	−44	35	−11	4.6	4.3	46	35	−15	4.4	4.1
	Operculum	−35	−7	18	3.8	3.6	55	−12	19	4.5	4.2
	Hippocampus	−33	−30	−11	3.3	3.2	23	−30	−15	3.5	3.4
	Amygdala	−30	−11	−18	3.1	3	24	−7	−11	3.7	3.6
ADHD+ < ADHD−	Hippocampus	−29	−37	−3	4.9	4.5	24	−36	0	4	3.7
	IPC	−59	−49	28	4.4	4.1					
T1-weighted grey matter—regression											
YGTSS											
Tourette syndrome—negative correlation	OFC	−3	33	−20	3.1	3					
	VLPFC	−41	21	−9	3.3	3.1	51	27	−6	3	2.9
PUTS											
Tourette syndrome—positive correlation	SI	−48	−13	33	4.7	4					
	PFC						19	24	43	4.2	3.7

Coordinates [*x*, *y*, *z*] refer to the Montreal Neurological Institute (MNI) standard stereotactic space.
IPC = inferior parietal cortex; MI = primary motor cortex; OFC = orbitofrontal cortex; PMd = dorsal premotor cortex; SI = primary somatosensory cortex; VLPFC = ventrolateral prefrontal cortex.

and humans, fractional anisotropy and mean diffusivity correlate linearly with the cumulative axonal membrane circumference and to a lesser extent with the amount of extra-axonal fraction and myelin thickness (Concha *et al.*, 2010). The supposition here is that the co-localized structural changes in functionally relevant areas result from increased processing demands due to premonitory sensations and their integration into repetitive motor patterns (Ferretti *et al.*, 2003). Alternatively, somatosensory cortex structural changes may arise as an adaptation to dysfunctional secondary somatosensory areas that show consistent grey matter volume/cortical thickness decreases in the parietal operculum bilaterally. The parietal operculum represents part of the secondary somatosensory areas and is involved in higher order functions focused on sensorimotor integration, attention and learning (Eickhoff *et al.*, 2007). We interpret the grey matter changes in these regions along our main hypothesis of structural fingerprint of disease persistence due to

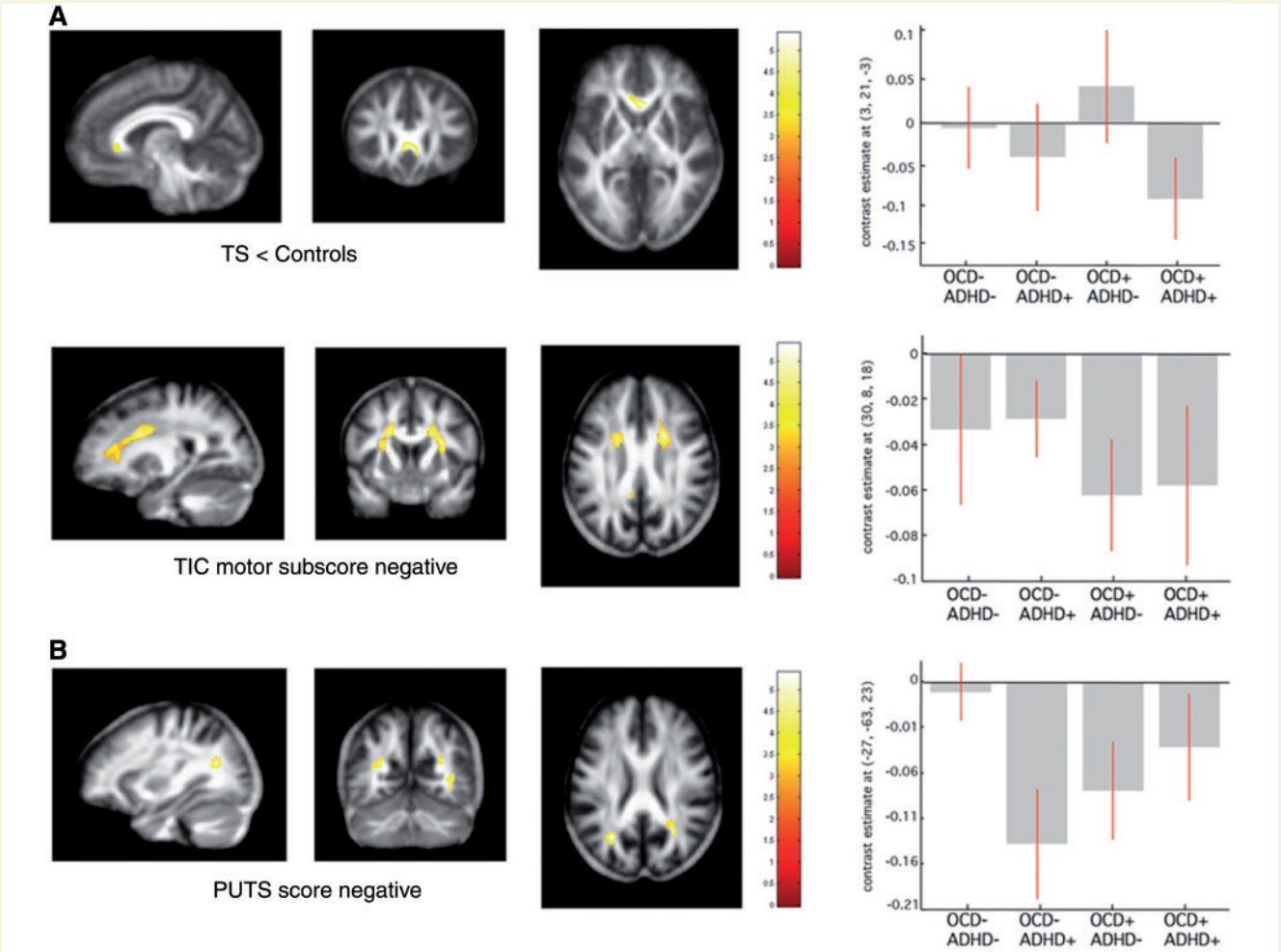

Figure 4 Statistical parametric maps of significant fractional anisotropy change in the Tourette syndrome cohort superimposed for presentation purposes at $P < 0.001$, uncorrected on T1-weighted image. *Right panel*: regression coefficients (betas) extracted from the voxel of maximum intensity over Tourette syndrome (TS) sub-groups depending on the presence (+) or absence (−) of co-morbidity OCD/ADHD. (**A**) Fractional anisotropy decreases in patients with Tourette syndrome compared with controls. (**B**) Fractional anisotropy reductions in patients with Tourette syndrome with symptom severity increase [motor tic sub-score, premonitory urge for tics score (PUTS)]. [*x*, *y*, *z*] coordinates refer to the Montreal Neurological Institute standardized space. Colour scales on the right indicate *t*-values.

suboptimal engagement of compensatory mechanisms. In our opinion, the convergent results from two independent data sets (T1-weighted and diffusion-weighted imaging) with symptom severity dependent grey matter volume increase and possible increase in cell density or axonal/dendritic arborization hindering water diffusion represent strong arguments against the assumption of Tourette syndrome related unidirectional cortical atrophy drawn from cortical thickness studies in children and adolescents (Sowell *et al.*, 2008; Fahim *et al.*, 2009).

Similarly to a previous VBM study in adults with Tourette syndrome (Ludolph *et al.*, 2006), we did not replicate earlier observations of structural differences within the midbrain (Garraux *et al.*, 2006), even at a very liberal statistical threshold. The assumption of reliable midbrain grey matter volume change detection is limited from a magnetic resonance physics and methodological perspective. Due to high iron content effectively shortening T1, mesencephalic structures and in particular the ventral tegmental area show reduced contrast from white matter in T1-weighted images. Accurate tissue classification is further limited by the very low probability of the presence of grey matter in this region in currently available tissue priors used for automated segmentation. Newly developed structural magnetic resonance imaging protocols have the potential to overcome these limitations (Helms *et al.*, 2009).

Affected white matter pathways

Inter-hemispheric connections

Due to the very low topo-anatomical specificity of white matter segments computed from T1-weighted images, we decided to obtain an independent diffusion-weighted imaging data set characterizing white matter tissue properties rather than just volume changes. We demonstrate regionally specific fractional anisotropy decreases in the genu of the corpus callosum, area connecting

orbitofrontal cortex and ventrolateral prefrontal cortex of both hemispheres (Park *et al.,* 2008). The dense fibre structure with radial orientation in this part of the corpus callosum allows for interpretation of fractional anisotropy reduction as a loss of connections. This is a finding that provides additional evidence for disruption of inter-hemispheric connections between affected nodes of the frontostriatal circuitry and replicates very recent results obtained with tract-based spatial statistics (Neuner *et al.,* 2010). Considering that our data processing strategy included scaling for both global and regional volume influences on diffusion-weighted imaging parameters, we can exclude previously described gross size changes in corpus callosum (Plessen *et al.,* 2004) having any impact on fractional anisotropy or mean diffusivity results.

Long associative pathways

Further exploration of white matter micro-structural integrity and its correlation with symptom severity in Tourette syndrome shows symmetric fractional anisotropy reductions in frontal parts of the superior longitudinal fascicles with motor tic increments. We detected a similar negative correlation between parietal portions of superior longitudinal fascicle and premonitory sensation intensity increases. The spatially selective change in fractional anisotropy along tracts connecting frontal and parietal areas can be interpreted in two ways. First, as suggested by a previous study showing unilateral fractional anisotropy decreases in the superior longitudinal fascicle comparing adults with Tourette syndrome and controls (Neuner *et al.,* 2010), it could reflect altered connectivity due to dysregulated myelination. The topo-anatomical specificity of our fractional anisotropy findings correlating with clinical scores describing distinct facets of Tourette syndrome allows for a more straightforward interpretation. In the absence of mean diffusivity changes, fractional anisotropy decreases can theoretically arise from local increases in the fraction of crossing fibres due to augmentation in cell density or axonal/dendritic arborizations that hinder water diffusion (Markham and Greenough, 2004; Kleim *et al.,* 2007). Frontal fractional anisotropy decrease in the superior longitudinal fascicle correlating with motor tic severity can be explained—by adaptive changes in frontostriatal pathways crossing the superior longitudinal fascicle; and for the parietal superior longitudinal fascicle portion can be explained with an expansion of projections to somatosensory cortex that are associated with greater premonitory urge intensity.

Modulation by co-morbidity

Our findings unmask the profound impact of OCD/ADHD co-morbidities on brain structure in Tourette syndrome demonstrating a specific topo-anatomical pattern, which overlaps with previously described alterations in the 'pure' forms of these disorders, but reversing the directionality of structural changes. One of two recent meta-analyses of VBM studies in adolescents and adults with 'pure' OCD found grey matter increases in orbitofrontal cortex, whereas both analyses confirmed grey matter increases in ventral and central portions of striatum (Radua and Mataix-Cols, 2009; Rotge *et al.,* 2010). Similarly to recent findings of a reversed pattern of cerebellar volume changes in children and adults with Tourette syndrome due to co-morbidity with OCD (Tobe *et al.,* 2010), we observe ventral striatal volume reduction with increasing obsessive-compulsive symptom severity assessed by the Leyton Obsessional Inventory score. Accordingly, our patients with Tourette syndrome with OCD and concomitant ADHD show orbitofrontal cortex grey matter reductions, thus reversing the pattern of cortical volume change described in 'pure' OCD.

The demonstrated grey matter volume reduction in hippocampus bilaterally and putamen volume increases in adults with Tourette syndrome with ADHD co-morbidity confirm the notion of overlap between disease related patterns in 'pure' ADHD and Tourette syndrome (Sowell *et al.,* 2003; Shaw and Rabin, 2009). It is noteworthy that we observe the greatest orbitofrontal cortex volume reduction in adults with Tourette syndrome when both OCD and ADHD co-morbidities are present. This underpins the notion that the orbitofrontal cortex is an important node within the Tourette syndrome 'matrix' representing a conjoint substrate for OCD/ADHD co-morbidity through its role as a processing bridge between emotion and cognition (Passingham *et al.,* 2002).

Underlying mechanisms

We used two complementary voxel-based morphometric techniques—voxel-based cortical thickness and VBM—to interpret our results. While a regional increase in cortical grey matter volume detected by VBM may be associated both with increased cortical thickness and changes in cortical folding, cortical thickness measures are thought to reflect 'pure' grey matter volume changes (Hutton *et al.,* 2008, 2009). The high correlation and substantial overlap of results from both methods allows us to conclude with confidence that Tourette syndrome-associated volume loss is due to real cortical thinning.

Our analysis of diffusion-weighted imaging parameters (fractional anisotropy and mean diffusivity) suggests possible tissue pathological mechanisms underlying grey and white matter changes detected in T1-weighted images. Although still an area of extensive research, mean diffusivity increases in grey matter in both healthy and diseased brains is believed to reflect the enlargement of extracellular space that is mainly associated with neuronal loss (Kantarci *et al.,* 2005; Carlesimo *et al.,* 2010). We observed parallel changes in volume and reciprocal mean diffusivity alterations in two nodes of the affected frontostriatal circuits in Tourette syndrome (e.g. orbitofrontal cortex, somatosensory cortex). This result can be interpreted as evidence for a bi-directional process of volume change driven by neuronal plasticity. Much less is known about the molecular/cellular substrate of fractional anisotropy changes. Therefore fractional anisotropy increases in the body of the caudate correlating with tics severity (YGTSS) should be interpreted with great caution.

Limitations

Some limitations of our study should be acknowledged. First, patient selection may not be fully representative of the general population of Tourette syndrome sufferers, since it targeted severely affected adults whose symptoms failed to remit during

adolescence. The interpretation of our findings in a specific subgroup of patients with Tourette syndrome is valid only under the assumption of a common pathophysiological mechanism underlying Tourette syndrome in childhood and adulthood.

Second, our subjects were not systematically assessed for other co-morbid psychopathologies of Tourette syndrome, such as personality disorders (Cavanna *et al.,* 2009). Recent VBM studies have highlighted abnormalities in fronto-limbic cortical areas of patients with borderline personality disorder (Minzenberg *et al.,* 2008; Soloff *et al.,* 2008; Brunner *et al.,* 2010), which is diagnosed in ~30% of patients with Tourette syndrome (Cavanna *et al.,* 2009). Although recent evidence questioned the specificity of these findings (Brunner *et al.,* 2010), future studies should clarify the relationship between co-morbid personality disorders and structural grey matter changes observed in adults with Tourette syndrome.

While aiming to dissociate the morphological characteristics of cortical changes with two morphometric techniques we can only speculate about their specific correlates at the cellular level. Both degenerative processes with cell loss, as well as changes in the proportion of neuronal/glial to extracellular components could contribute to magnetic resonance signal intensity differences we describe. Combining morphometry results based on T1-weighted data with diffusion-weighted imaging parameter maps directly related to tissue properties at the cellular level offers a unique opportunity for understanding underlying pathophysiological mechanisms. The challenge from the methodological point of view when using VBM for group comparisons is the necessary adjustment for regional and global volume differences.

Conclusion

To our knowledge, this is the first study in adult patients with Tourette syndrome presenting results from independent neuroimaging data sets (i.e. T1-weighted and diffusion-weighted imaging) that use complementary computational anatomy methods (i.e. VBM and voxel-based cortical thickness) aimed at performing a detailed assessment of brain structure. The spatial pattern of structural changes in our study showing substantial overlap with previous reports in children and adolescents with Tourette syndrome supports the notion that the condition persists into adulthood due to suboptimal adaptation (Plessen *et al.,* 2009). The temporal dynamics of structural brain changes in Tourette syndrome suggests parallel engagement of plastic compensatory process throughout childhood and adolescence within and beyond the primarily affected functional circuitry.

Future prospective studies at multiple scan time-points should depict the trajectory of structural brain changes between childhood and adulthood to clarify the pathophysiological mechanisms underlying disease persistence in adults with Tourette syndrome.

Acknowledgements

We thank all the participants in our study and the radiographers at the Functional Imaging Laboratory for their assistance acquiring the data.

Funding

Wellcome Trust Grant (ref: 075696/Z/04/Z to R.S.F., S. Tabrizi and J. Ashburner).

Supplementary material

Supplementary material is available at *Brain* online.

References

Albin RL, Mink JW. Recent advances in Tourette syndrome research. Trends Neurosci 2006; 29: 175–82.

Alexander GE, Crutcher MD, DeLong MR. Basal ganglia-thalamocortical circuits: parallel substrates for motor, oculomotor, "prefrontal" and "limbic" functions. Prog Brain Res 1990; 85: 119–46.

Aron AR, Fletcher PC, Bullmore ET, Sahakian BJ, Robbins TW. Stop-signal inhibition disrupted by damage to right inferior frontal gyrus in humans. Nat Neurosci 2003; 6: 115–6.

Ashburner J. A fast diffeomorphic image registration algorithm. Neuroimage 2007; 38: 95–113.

Ashburner J, Csernansky JG, Davatzikos C, Fox NC, Frisoni GB, Thompson PM. Computer-assisted imaging to assess brain structure in healthy and diseased brains. Lancet Neurol 2003; 2: 79–88.

Ashburner J, Friston KJ. Unified segmentation. Neuroimage 2005; 26: 839–51.

Basser PJ, Mattiello J, LeBihan D. Estimation of the effective self-diffusion tensor from the NMR spin echo. J Magn Reson B 1994; 103: 247–54.

Baym CL, Corbett BA, Wright SB, Bunge SA. Neural correlates of tic severity and cognitive control in children with Tourette syndrome. Brain 2008; 131: 165–79.

Bloch MH, Leckman JF. Clinical course of Tourette syndrome. J Psychosom Res 2009; 67: 497–501.

Bloch MH, Leckman JF, Zhu H, Peterson BS. Caudate volumes in childhood predict symptom severity in adults with Tourette syndrome. Neurology 2005; 65: 1253–8.

Bohlhalter S, Goldfine A, Matteson S, Garraux G, Hanakawa T, Kansaku K, et al. Neural correlates of tic generation in Tourette syndrome: an event-related functional MRI study. Brain 2006; 129 (Pt 8): 2029–37.

Brunner R, Henze R, Parzer P, Kramer J, Feigl N, Lutz K, et al. Reduced prefrontal and orbitofrontal gray matter in female adolescents with borderline personality disorder: is it disorder specific? Neuroimage 2010; 49: 114–20.

Carlesimo GA, Cherubini A, Caltagirone C, Spalletta G. Hippocampal mean diffusivity and memory in healthy elderly individuals: a cross-sectional study. Neurology 2010; 74: 194–200.

Cavanna AE, Servo S, Monaco F, Robertson MM. The behavioral spectrum of Gilles de la Tourette syndrome. J Neuropsychiatry Clin Neurosci 2009; 21: 13–23.

Concha L, Livy DJ, Beaulieu C, Wheatley BM, Gross DW. In vivo diffusion tensor imaging and histopathology of the fimbria-fornix in temporal lobe epilepsy. J Neurosci 2010; 30: 996–1002.

Cook PA, Zhang H, Avants BB, Yushkevich P, Alexander DC, Gee JC, et al. An automated approach to connectivity-based partitioning of brain structures. Med Image Comput Comput Assist Interv Int Conf Med Image Comput Comput Assist Interv 2005; 8 (Pt 1): 164–71.

Cooper J. The Leyton obsessional inventory. Psychol Med 1970; 1: 48–64.

Draganski B, Kherif F, Kloppel S, Cook PA, Alexander DC, Parker GJ, et al. Evidence for segregated and integrative connectivity patterns in the human Basal Ganglia. J Neurosci 2008; 28: 7143–52.

Eickhoff SB, Grefkes C, Zilles K, Fink GR. The somatotopic organization of cytoarchitectonic areas on the human parietal operculum. Cereb Cortex 2007; 17: 1800–11.

Eickhoff SB, Stephan KE, Mohlberg H, Grefkes C, Fink GR, Amunts K, et al. A new SPM toolbox for combining probabilistic cytoarchitectonic maps and functional imaging data. Neuroimage 2005; 25: 1325–35.

Fahim C, Yoon U, Sandor P, Frey K, Evans AC. Thinning of the motor-cingulate-insular cortices in siblings concordant for Tourette syndrome. Brain Topogr 2009; 22: 176–84.

Ferretti A, Babiloni C, Gratta CD, Caulo M, Tartaro A, Bonomo L, et al. Functional topography of the secondary somatosensory cortex for nonpainful and painful stimuli: an fMRI study. Neuroimage 2003; 20: 1625–38.

Fischl B, Sereno MI, Dale AM. Cortical surface-based analysis. II: inflation, flattening, and a surface-based coordinate system. Neuroimage 1999; 9: 195–207.

Friston KJ. Testing for anatomically specified regional effects. Hum Brain Mapp 1997; 5: 133–6.

Friston KJ, Tononi G, Reeke GN Jr, Sporns O, Edelman GM. Value-dependent selection in the brain: simulation in a synthetic neural model. Neuroscience 1994; 59: 229–43.

Garraux G, Goldfine A, Bohlhalter S, Lerner A, Hanakawa T, Hallett M. Increased midbrain gray matter in Tourette's syndrome. Ann Neurol 2006; 59: 381–5.

Gerard E, Peterson BS. Developmental processes and brain imaging studies in Tourette syndrome. J Psychosom Res 2003; 55: 13–22.

Good CD, Johnsrude I, Ashburner J, Henson RN, Friston KJ, Frackowiak RS. Cerebral asymmetry and the effects of sex and handedness on brain structure: a voxel-based morphometric analysis of 465 normal adult human brains. Neuroimage 2001; 14: 685–700.

Haber SN, Knutson B. The reward circuit: linking primate anatomy and human imaging. Neuropsychopharmacology 2010; 35: 4–26.

Helms G, Draganski B, Frackowiak R, Ashburner J, Weiskopf N. Improved segmentation of deep brain grey matter structures using magnetization transfer (MT) parameter maps. Neuroimage 2009; 47: 194–8.

Hesslinger B, Tebartz van Elst L, Thiel T, Haegele K, Hennig J, Ebert D. Frontoorbital volume reductions in adult patients with attention deficit hyperactivity disorder. Neurosci Lett 2002; 328: 319–21.

Hutton C, De Vita E, Ashburner J, Deichmann R, Turner R. Voxel-based cortical thickness measurements in MRI. Neuroimage 2008; 40: 1701–10.

Hutton C, Draganski B, Ashburner J, Weiskopf N. A comparison between voxel-based cortical thickness and voxel-based morphometry in normal aging. Neuroimage 2009; 48: 371–80.

Josse G, Seghier ML, Kherif F, Price CJ. Explaining function with anatomy: language lateralization and corpus callosum size. J Neurosci 2008; 28: 14132–9.

Kantarci K, Petersen RC, Boeve BF, Knopman DS, Weigand SD, O'Brien PC, et al. DWI predicts future progression to Alzheimer disease in amnestic mild cognitive impairment. Neurology 2005; 64: 902–4.

Kleim JA, Kleim ED, Cramer SC. Systematic assessment of training-induced changes in corticospinal output to hand using frameless stereotaxic transcranial magnetic stimulation. Nat Protoc 2007; 2: 1675–84.

Leckman JF, Riddle MA, Hardin MT, Ort SI, Swartz KL, Stevenson J, et al. The Yale Global Tic Severity Scale: initial testing of a clinician-rated scale of tic severity. J Am Acad Child Adolesc Psychiatry 1989; 28: 566–73.

Lee JE, Chung MK, Lazar M, DuBray MB, Kim J, Bigler ED, et al. A study of diffusion tensor imaging by tissue-specific, smoothing-compensated voxel-based analysis. Neuroimage 2009; 44: 870–83.

Ludolph AG, Juengling FD, Libal G, Ludolph AC, Fegert JM, Kassubek J. Grey-matter abnormalities in boys with Tourette syndrome: magnetic resonance imaging study using optimised voxel-based morphometry. Br J Psychiatry 2006; 188: 484–5.

Makki MI, Govindan RM, Wilson BJ, Behen ME, Chugani HT. Altered fronto-striato-thalamic connectivity in children with Tourette syndrome assessed with diffusion tensor MRI and probabilistic fiber tracking. J Child Neurol 2009; 24: 669–78.

Markham JA, Greenough WT. Experience-driven brain plasticity: beyond the synapse. Neuron Glia Biol 2004; 1: 351–63.

Mazzone L, Yu S, Blair C, Gunter BC, Wang Z, Marsh R, et al. An fMRI study of frontostriatal circuits during the inhibition of eye blinking in persons with Tourette syndrome. Am J Psychiatry 2010; 167: 341–9.

Mink JW. The basal ganglia and involuntary movements: impaired inhibition of competing motor patterns. Arch Neurol 2003; 60: 1365–8.

Minzenberg MJ, Fan J, New AS, Tang CY, Siever LJ. Frontolimbic structural changes in borderline personality disorder. J Psychiatr Res 2008; 42: 727–33.

Muller-Vahl KR, Kaufmann J, Grosskreutz J, Dengler R, Emrich HM, Peschel T. Prefrontal and anterior cingulate cortex abnormalities in Tourette syndrome: evidence from voxel-based morphometry and magnetization transfer imaging. BMC Neurosci 2009; 10: 47.

Neuner I, Kupriyanova Y, Stocker T, Huang R, Posnansky O, Schneider F, et al. White-matter abnormalities in Tourette syndrome extend beyond motor pathways. Neuroimage 2010; 51: 1184–93.

O'Doherty JP, Hampton A, Kim H. Model-based fMRI and its application to reward learning and decision making. Ann NY Acad Sci 2007; 1104: 35–53.

Palminteri S, Lebreton M, Worbe Y, Grabli D, Hartmann A, Pessiglione M. Pharmacological modulation of subliminal learning in Parkinson's and Tourette's syndromes. Proc Natl Acad Sci USA 2009; 106: 19179–84.

Parent A, Hazrati LN. Functional anatomy of the basal ganglia. I. The cortico-basal ganglia-thalamo-cortical loop. Brain Res Brain Res Rev 1995; 20: 91–127.

Park HJ, Kim JJ, Lee SK, Seok JH, Chun J, Kim DI, et al. Corpus callosal connection mapping using cortical gray matter parcellation and DT-MRI. Hum Brain Mapp 2008; 29: 503–16.

Passingham RE, Stephan KE, Kotter R. The anatomical basis of functional localization in the cortex. Nat Rev Neurosci 2002; 3: 606–16.

Peterson B, Riddle MA, Cohen DJ, Katz LD, Smith JC, Hardin MT, et al. Reduced basal ganglia volumes in Tourette's syndrome using three-dimensional reconstruction techniques from magnetic resonance images. Neurology 1993; 43: 941–9.

Peterson BS, Choi HA, Hao X, Amat JA, Zhu H, Whiteman R, et al. Morphologic features of the amygdala and hippocampus in children and adults with Tourette syndrome. Arch Gen Psychiatry 2007; 64: 1281–91.

Peterson BS, Skudlarski P, Anderson AW, Zhang H, Gatenby JC, Lacadie CM, et al. A functional magnetic resonance imaging study of tic suppression in Tourette syndrome. Arch Gen Psychiatry 1998; 55: 326–33.

Peterson BS, Staib L, Scahill L, Zhang H, Anderson C, Leckman JF, et al. Regional brain and ventricular volumes in Tourette syndrome. Arch Gen Psychiatry 2001; 58: 427–40.

Peterson BS, Thomas P, Kane MJ, Scahill L, Zhang H, Bronen R, et al. Basal Ganglia volumes in patients with Gilles de la Tourette syndrome. Arch Gen Psychiatry 2003; 60: 415–24.

Plessen KJ, Bansal R, Peterson BS. Imaging evidence for anatomical disturbances and neuroplastic compensation in persons with Tourette syndrome. J Psychosom Res 2009; 67: 559–73.

Plessen KJ, Wentzel-Larsen T, Hugdahl K, Feineigle P, Klein J, Staib LH, et al. Altered interhemispheric connectivity in individuals with Tourette's disorder. Am J Psychiatry 2004; 161: 2028–37.

Radua J, Mataix-Cols D. Voxel-wise meta-analysis of grey matter changes in obsessive-compulsive disorder. Br J Psychiatry 2009; 195: 393–402.

Ramus SJ, Davis JB, Donahue RJ, Discenza CB, Waite AA. Interactions between the orbitofrontal cortex and the hippocampal memory system

during the storage of long-term memory. Ann NY Acad Sci 2007; 1121: 216–31.

Raz A, Zhu H, Yu S, Bansal R, Wang Z, Alexander GM, et al. Neural substrates of self-regulatory control in children and adults with Tourette syndrome. Can J Psychiatry 2009; 54: 579–88.

Reese TG, Heid O, Weisskoff RM, Wedeen VJ. Reduction of eddy-current-induced distortion in diffusion MRI using a twice-refocused spin echo. Magn Reson Med 2003; 49: 177–82.

Robertson MM. Tourette syndrome, associated conditions and the complexities of treatment. Brain 2000; 123 (Pt 3): 425–62.

Rotge JY, Langbour N, Guehl D, Bioulac B, Jaafari N, Allard M, et al. Gray matter alterations in obsessive-compulsive disorder: an anatomic likelihood estimation meta-analysis. Neuropsychopharmacology 2010; 35: 686–91.

Schultz W. Neural coding of basic reward terms of animal learning theory, game theory, microeconomics and behavioural ecology. Curr Opin Neurobiol 2004; 14: 139–47.

Serrien DJ, Orth M, Evans AH, Lees AJ, Brown P. Motor inhibition in patients with Gilles de la Tourette syndrome: functional activation patterns as revealed by EEG coherence. Brain 2005; 128 (Pt 1): 116–25.

Shaw P, Rabin C. New insights into attention-deficit/hyperactivity disorder using structural neuroimaging. Curr Psychiatry Rep 2009; 11: 393–8.

Singer HS. Tourette's syndrome: from behaviour to biology. Lancet Neurol 2005; 4: 149–59.

Soloff P, Nutche J, Goradia D, Diwadkar V. Structural brain abnormalities in borderline personality disorder: a voxel-based morphometry study. Psychiatry Res 2008; 164: 223–36.

Sowell ER, Kan E, Yoshii J, Thompson PM, Bansal R, Xu D, et al. Thinning of sensorimotor cortices in children with Tourette syndrome. Nat Neurosci 2008; 11: 637–9.

Sowell ER, Thompson PM, Welcome SE, Henkenius AL, Toga AW, Peterson BS. Cortical abnormalities in children and adolescents with attention-deficit hyperactivity disorder. Lancet 2003; 362: 1699–707.

Thomalla G, Siebner HR, Jonas M, Baumer T, Biermann-Ruben K, Hummel F, et al. Structural changes in the somatosensory system correlate with tic severity in Gilles de la Tourette syndrome. Brain 2009; 132 (Pt 3): 765–77.

Tobe RH, Bansal R, Xu D, Hao X, Liu J, Sanchez J, et al. Cerebellar morphology in Tourette syndrome and obsessive-compulsive disorder. Ann Neurol 2010; 67: 479–87.

Tzourio-Mazoyer N, Landeau B, Papathanassiou D, Crivello F, Etard O, Delcroix N, et al. Automated anatomical labeling of activations in SPM using a macroscopic anatomical parcellation of the MNI MRI single-subject brain. Neuroimage 2002; 15: 273–89.

Wang L, Lee DY, Bailey E, Hartlein JM, Gado MH, Miller MI, et al. Validity of large-deformation high dimensional brain mapping of the basal ganglia in adults with Tourette syndrome. Psychiatry Res 2007; 154: 181–90.

Wheeler-Kingshott CA, Parker GJ, Symms MR, Hickman SJ, Tofts PS, Miller DH, et al. ADC mapping of the human optic nerve: increased resolution, coverage, and reliability with CSF-suppressed ZOOM-EPI. Magn Reson Med 2002; 47: 24–31.

Winkler AM, Kochunov P, Blangero J, Almasy L, Zilles K, Fox PT, et al. Cortical thickness or grey matter volume? The importance of selecting the phenotype for imaging genetics studies. Neuroimage 2010; 53: 1135–46.

Woods DW, Piacentini J, Himle MB, Chang S. Premonitory urge for tics scale (PUTS): initial psychometric results and examination of the premonitory urge phenomenon in youths with Tic disorders. J Dev Behav Pediatr 2005; 26: 397–403.

Worsley KJ, Marrett S, Neelin P, Vandal AC, Friston KJ, Evans AC. A unified statistical approach for determining significant signals in images of cerebral activation. Hum Brain Mapp 1996; 4: 58–73.